J|A|C|S
ARTICLES
Published on Web 05/03/2006

Spontaneous Transformation of CdTe Nanoparticles into Angled Te Nanocrystals: From Particles and Rods to Checkmarks, X-Marks, and Other Unusual Shapes

Zhiyong Tang,[†] Ying Wang,[‡] Sachin Shanbhag,[†] Michael Giersig,[§] and Nicholas A. Kotov*[,†,‡]

Department of Chemical Engineering and Department of Material Science and Engineering, 2300 Hayward, H. H. Dow Bldg, University of Michigan, Ann Arbor, Michigan 48109-2136, U.S.A., and Center of Advanced European Studies and Research, CEASAR, 53175 Bonn, Germany

Received December 22, 2005; E-mail: kotov@umich.edu

Abstract: CdTe nanoparticles spontaneously transform into the branched Te nanocrystals with the unique, highly anisotropic shape of checkmarks after partial removal of the stabilizers of L-cysteine. The Te checkmarks are made in a relatively high yield and uniformity; the length of the arms is ca. 150 nm, whereas the angle between the arms is 74°. Subsequent growth of the particle yields mothlike nanocrystals retaining geometrical anisotropy. Unlike the previous synthesis methods of branched nanocrystals, they are formed via a merger of individual rod-shaped crystallites. High-energy crystal faces on their apexes act as the sticky points causing the particles to join in the ends. This is the first demonstration of spontaneous transformation of binary semiconductor particles into highly anisotropic nanocolloids in an angled conformation. The end reactivity of starting Te rods can be used both for bottom-up fabrication of nanoscale electronics and relatively safe and nontoxic method of synthesis of Te-based optical and other materials.

Introduction

Nanocrystals (NCs) with nonspherical shapes are becoming more common in nanoscale synthesis.[1−3] The desire to control the direction of flow of different forms of energy in nanomaterials makes any synthetic methods leading to nonspherical, branched, or noncentrosymmetric crystals of special interest because the geometrical uniqueness of nanocolloids translates into similarly unique behavior in chemical, optical, and electronic senses.[4] Self-organization of these species driven by strongly anisotropic interparticle interactions can be a source of inspiration both for a preparation of analogue electronic devices as well as the development of new methods of their structural selection. Potentially gigantic nonlinear optical properties, for instance negative refraction index structures, and other photonic and electronic properties[5,6] of such systems can be behind immediately practical reasoning for the synthesis of particles with nonconventional shapes. The family of nonspherical nanocolloids typically includes one-dimensional (1D) nanowires or nanotubes,[2,7,8] two-dimensional (2D) nanodisks or nanoprism,[9−12] and branched nanobipods, nanotripods, nanotetrapods, nanopentapods, and nanohexapods.[13−15] They are commonly made by controlling the rate of growth of different faces of crystals in solution. In this way, branched NCs from CdSe,[13] and different types of other materials including CdS,[16] CdSe,[17] CdTe,[18] PbS,[19] PbSe,[20] ZnSe,[21] MnS,[22] TiO_2,[23,24]

[†] Department of Chemical Engineering, University of Michigan.
[‡] Department of Material Science and Engineering, University of Michigan.
[§] Center of Advanced European Studies and Research.

(1) Alivisatos, A. P. *Science* **1996**, *271*, 933−937.
(2) Xia, Y.; Yang, P.; Sun, Y.; Wu, Y.; Mayers, B.; Gates, B.; Yin, Y.; Kim, F.; Yan, H. *Adv. Mater.* **2003**, *15*, 353−389.
(3) Jun, Y. w.; Lee, J. H.; Choi, J. S.; Cheon, J. *J. Phys. Chem. B* **2005**, *109*, 14795−14806.
(4) Narayanan, R.; El Sayed, M. A. *J. Phys. Chem. B* **2005**, *109*, 12663−12676.
(5) Hao, E.; Schatz, G. C.; Hupp, J. T. *J. Fluoresc.* **2004**, *14*, 331−341.
(6) Li, J.; Wang, L. W. *Nano Lett.* **2003**, *3*, 1357−1363.
(7) Peng, X.; Manna, U.; Yang, W.; Wickham, J.; Scher, E.; Kadavanich, A.; Allvisatos, A. P. *Nature* **2000**, *404*, 59−61.
(8) Sau, T. K.; Murphy, C. J. *Langmuir* **2004**, *20*, 6414−6420.
(9) Puntes, V. F.; Zanchet, D.; Erdonmez, C. K.; Alivisatos, A. P. *J. Am. Chem. Soc.* **2002**, *124*, 12874−12880.
(10) Jin, R.; Cao, Y. C.; Hao, E.; Metraux, G. S.; Schatz, G. C.; Mirkin, C. A. *Nature* **2003**, *425*, 487−490.
(11) Pastoriza-Santos, I.; Liz-Marzan, L. M. *Nano Lett.* **2002**, *2*, 903−905.
(12) Pinna, N.; Garnweitner, G.; Beato, P.; Niederberger, M.; Antonietti, M. *Small* **2005**, *1*, 112−121.
(13) Manna, L.; Scher, E. C.; Alivisatos, A. P. *J. Am. Chem. Soc.* **2000**, *122*, 12700−12706.
(14) Chen, S.; Wang, Z. L.; Ballato, J.; Foulger, S. H.; Carroll, D. L. *J. Am. Chem. Soc.* **2003**, *125*, 16186−16187.
(15) Zitoun, D.; Pinna, N.; Frolet, N.; Belin, C. *J. Am. Chem. Soc.* **2005**, *127*, 15034−15035.
(16) Jun, Y. w.; Lee, S. M.; Kang, N. J.; Cheon, J. *J. Am. Chem. Soc.* **2001**, *123*, 5150−5151.
(17) Peng, Z. A.; Peng, X. *J. Am. Chem. Soc.* **2002**, *124*, 3343−3353.
(18) Manna, L.; Milliron, D. J.; Meisel, A.; Scher, E. C.; Alivisatos, A. P. *Nat. Mater.* **2003**, *2*, 382−385.
(19) Lee, S. M.; Jun, Y. w.; Cho, S. N.; Cheon, J. *J. Am. Chem. Soc.* **2002**, *124*, 11244−11245.
(20) Cho, K. S.; Talapin, D. V.; Gaschler, W.; Murray, C. B. *J. Am. Chem. Soc.* **2005**, *127*, 7140−7147.
(21) Cozzoli, P. D.; Manna, L.; Curri, M. L.; Kudera, S.; Giannini, C.; Striccoli, M.; Agostiano, A. *Chem. Mater.* **2005**, *17*, 1296−1306.
(22) Jun, Y. w.; Jung, Y. y.; Cheon, J. *J. Am. Chem. Soc.* **2002**, *124*, 615−619.
(23) Jun, Y. w.; Casula, M. F.; Sim, J. H.; Kim, S. Y.; Cheon, J.; Alivisatos, A. P. *J. Am. Chem. Soc.* **2003**, *125*, 15981−15985.
(24) Polleux, J.; Pinna, N.; Antonietti, M.; Niederberger, M. *Adv. Mater.* **2004**, *16*, 436−439.

10.1021/ja0582096 CCC: $33.50

MnO,[15] WO_3,[25] Au,[14,26,27] Ag,[28] Rh,[29] and Pt,[30−32] have been obtained. The large variety of materials from which the branched metal and semiconductor NCs have been made is a measure of the success of this approach. However, it also has its limitations originating in intrinsic symmetries of crystal lattices. Can one obtain branched NCs in some other ways?

Recently, several self-organization mechanisms were found to occur between nanoparticles (NPs).[33−37] In this context and within the limits of this publication, NPs are referred to as objects comprised within nanoscale with apparent isotropic geometry to distinguish them from anisotropic NCs. One example of such processes is the self-assembly of NPs into nanochains and nanowires occurring upon destabilization of NPs after partial removal of the protective organic coating.[38−40] The synthetic approaches beginning with destabilized NPs have an interesting advantage in unordinary and rather unexpected behavior of such nanocolloids. This feature originates from a manifold of long- and short-range of interparticle forces brought about by partial removal of the stabilizer shell. Correspondingly, one should expect markedly different products of their chemical transformations from those studied before. Regardless of the material, self-organization processes of partially destabilized NPs have high fundamental importance because they will help to understand the interactions at the nanoscale and can lead to rather out-of-the-box fabrication procedures for nanoscale materials and devices.[33−37] In this article, the spontaneous transformation process starting from destabilized CdTe NPs and producing branched Te NCs with unique anisotropic structure is described. Unlike some other nanoscale self-organization processes, this takes place with a nanocolloid formed in situ, i.e., preceded by initial chemical reactions. The importance of nonspherical Te-based nanomaterials, especially those with relevance to nanoscale optoelectronics, is hard to overestimate. Angled checkmark- and moth-like NCs as well as related shapes have not been obtained before and can inspire preparation of similar geometric systems from other materials or can further self-assemble into superstructures of higher levels of complexity and functionality.

Experimental Section

The synthesis of water-soluble L-cysteine-stabilized CdTe NPs followed the recipe described in the publications.[44−46] In brief, H_2Te gas (generated by the reaction of 0.2 g Al_2Te_3 lumps with 15 mL of 0.5 M H_2SO_4 under N_2 atmosphere) was passed through to a nitrogen-saturated $Cd(ClO_4)_2 \cdot 6H_2O$ aqueous solution (0.013 M, 125 mL) at pH 11.2 in the presence of L-cysteine (691 mg) as a stabilizing agent. The reaction mixture was refluxed under N_2 gas for different periods of time to obtain NPs with desirable sizes. For instance, CdTe NPs with average diameters of 3.5 nm were prepared after 40 min reflux; NPs with diameters of 5.0 nm were produced after 12 h reflux. The final atomic concentration of Te in the solution was 3.6 mM.

2-Propanol (5 mL) was added into 5 mL of L-cysteine-stabilized CdTe crude product NP solution, and the solution immediately became turbid. After centrifugation at 6000 rpm for 10 min, the precipitates of CdTe NPs were obtained. The spontaneous transformation process was performed by redispersing CdTe precipitates into 5 mL of pH 9 solution containing 4 mM ethylenediaminetetraacetic acid dipotassium salt dehydrate (EDTA). The reaction solution, while undergoing the spontaneous transformation, was kept in the dark under ambient conditions.

Results and Discussion

The starting point for the synthesis here was the 3.5 nm CdTe NPs stabilized with L-cysteine with photoluminescence (PL) maximum at 580 nm. Similarly to our previous report,[38] the depletion of the stabilizer shell of the colloid was achieved by the addition of methanol or 2-propanol as an antisolvent into the NP solutions and subsequent centrifugation. After that, the precipitates of stabilizer-depleted CdTe NPs were redispersed into 4 mM EDTA solution at pH 9. High pH of an EDTA solution maintained negative charges on the NP surfaces and, thus, prevented aggregation from dipolar or van der Waals attraction. The elemental analysis from energy-dispersed X-ray spectrometry indicates that the ratio between Cd and S in NPs increases from 0.9 to 4.0 after the process of methanol precipitation and redissolution, which proves the partial removal of stabilizers via the above process. During the synthetic process, the color of the stabilizer-depleted CdTe solution changed from orange to blue after 15 days in the presence of EDTA.

EDTA also destabilizes CdTe NPs as compared to thiolic shells. Both destabilization procedures were a prerequisite to achieve anisotropic Te NCs. For example, if EDTA compounds were directly added into the crude CdTe NP solution without the step of stabilizer depletion, the transformation products were composed of anisotropic Te nanorods and CdTeS alloy NPs because an excessive amount of L-cysteine stabilizers also involved the spontaneous transformation reaction. The detailed study on the formation of CdTeS alloy NPs is being reported in a separate paper.[47]

Structure of the Produced Nanocolloids. Transmission electronic microscopy (TEM) reveals that the spontaneous transformation products of CdTe NPs are exclusively anisotropic NCs (Figure 1A), whose shapes include 46% rods (Figure 1B), 18% checkmarks (Figure 1C), and 36% moths (Figure 1D).

(25) Polleux, J.; Pinna, N.; Antonietti, M.; Niederberger, M. *J. Am. Chem. Soc.* **2005**, *127*, 15595−15601.
(26) Hao, E.; Bailey, R. C.; Schatz, G. C.; Hupp, J. T.; Li, S. *Nano Lett.* **2004**, *4*, 327−330.
(27) Sau, T. K.; Murphy, C. J. *J. Am. Chem. Soc.* **2004**, *126*, 8648−8649.
(28) Sanedrin, R. G.; Georganopoulou, D. G.; Park, S.; Mirkin, C. A. *Adv. Mater. (Weinheim, Ger.)* **2005**, *17*, 1027−1031.
(29) Hoefelmeyer, J. D.; Niesz, K.; Somorjai, G. A.; Tilley, T. D. *Nano Lett.* **2005**, *5*, 435−438.
(30) Herricks, T.; Chen, J.; Xia, Y. *Nano Lett.* **2004**, *4*, 2367−2371.
(31) Teng, X.; Yang, H. *Nano Lett.* **2005**, *5*, 885−891.
(32) Chen, J.; Herricks, T.; Xia, Y. *Angew. Chem., Int. Ed.* **2005**, *44*, 2589−2592.
(33) Murray, C. B.; Kagan, C. R.; Bawendi, M. G. *Ann. Rev. Mater. Sci.* **2000**, *30*, 545−610.
(34) Pileni, M. P. *J. Phys. Chem. B* **2001**, *105*, 3358−3371.
(35) Rogach, A. L.; Talapin, D. V.; Shevchenko, E. V.; Kornowski, A.; Haase, M.; Weller, H. *Adv. Funct. Mater.* **2002**, *12*, 653−664.
(36) Tang, Z.; Kotov, N. A. *Adv. Mater.* **2005**, *17*, 951−962.
(37) Kurth, D. G.; Lehmann, P.; Lesser, C. *Chem. Commun.* **2000**, *11*, 949−950.
(38) Tang, Z.; Kotov, N. A.; Giersig, M. *Science* **2002**, *297*, 237−240.
(39) Tang, Z.; Ozturk, B.; Wang, Y.; Kotov, N. A. *J. Phys. Chem. B* **2004**, *108*, 6927−6931.
(40) Tang, Z.; Wang, Y.; Sun, K.; Kotov, N. A. *Adv. Mater.* **2005**, *17*, 358−363.
(41) Mayers, B.; Gates, B.; Yin, Y.; Xia, Y. *Adv. Mater.* **2001**, *13*, 1380−1384.
(42) Mayers, B.; Xia, Y. *J. Mater. Chem.* **2002**, *12*, 1875−1881.
(43) Mayers, B.; Xia, Y. *Adv. Mater.* **2002**, *14*, 279−282.
(44) Mamedova, N. N.; Kotov, N. A.; Rogach, A. L.; Studer, J. *Nano Lett.* **2001**, *1*, 281−286.
(45) Gaponik, N.; Talapin, D. V.; Rogach, A. L.; Hoppe, K.; Shevchenko, E. V.; Kornowski, A.; Eychmueller, A.; Weller, H. *J. Phys. Chem. B* **2002**, *106*, 7177−7185.
(46) Talapin, D. V.; Haubold, S.; Rogach, A. L.; Kornowski, A.; Haase, M.; Weller, H. A. *J. Phys. Chem. B* **2001**, *105*, 2260−2263.
(47) Tang, Z.; Wang, Y.; Podsiadlo, P.; Kotov, N. A. *J. Am. Chem. Soc.*, **2006**, JA055366W, in press.

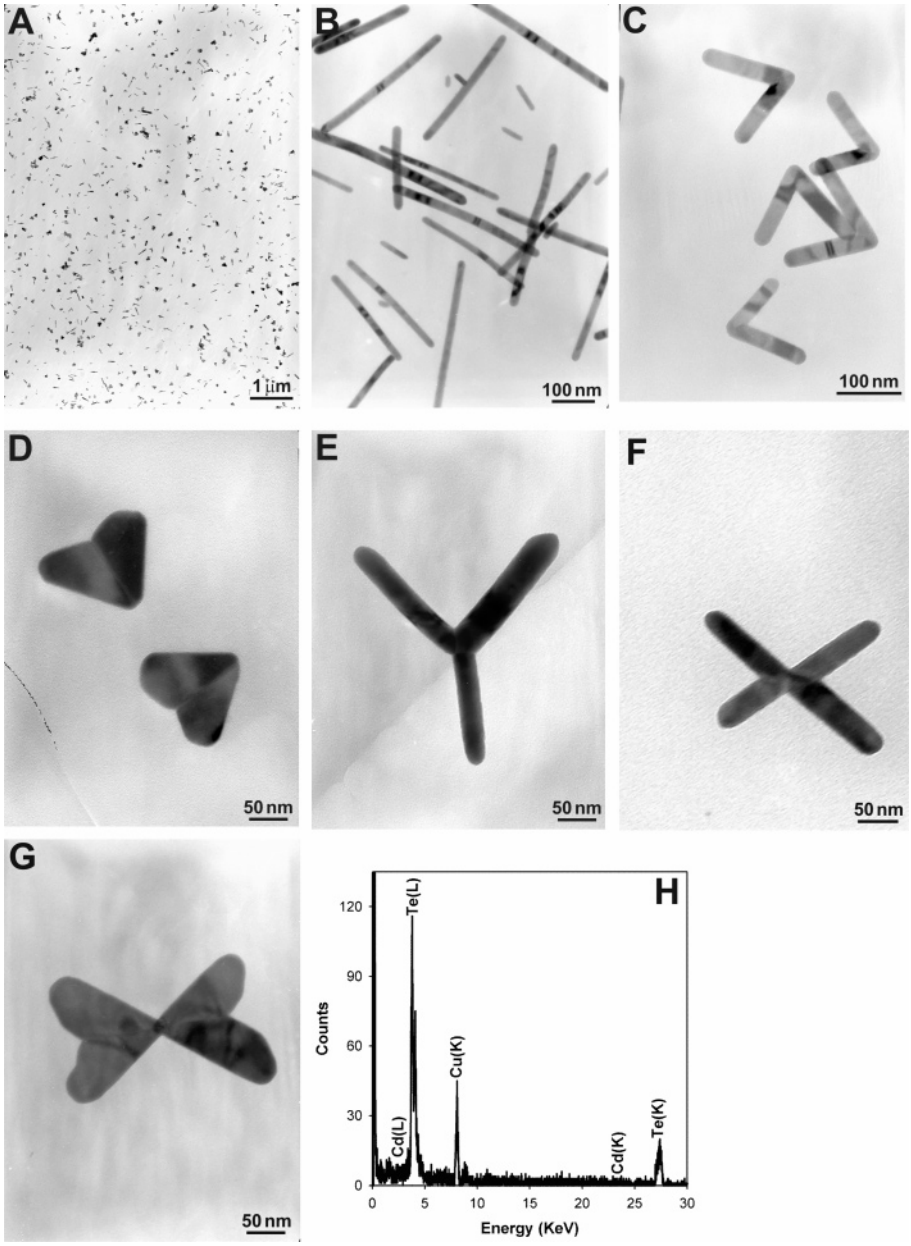

Figure 1. (A) TEM images of the spontaneous transformation products of CdTe NPs. TEM images of (B) nanorods, (C) nanocheckmarks, (D) nanomoths, (E) Y-shaped, and (F) and (G) X-shaped. (H) EDX spectrum of the products. The signals of Cu detected in EDX should be attributed to TEM grids.

Occasionally, NCs having shapes of Y-marks (Figure 1E) or X-marks (Figure 1F,G) have been observed. Because the appearance frequency of Ys and Xs is low, we intentionally limit the discussion of these shapes at this point of the study until we understand completely the reaction of checkmark formation. Nevertheless, they may serve as examples of more complex products that can be formed from nanoscale building blocks (see below). Elemental analysis from energy-dispersed X-ray spectrum (EDX) shows that all the products are made from Te rather than CdTe (Figure 1H). The Te nanorods have an average diameter of 17 nm with the length varying from 30 to 400 nm (Figure 1B). The size of Te nanoscale checkmarks is more uniform. For instance, the length and width of all arms in different Te NCs is 150 ± 20 nm and 30 ± 3 nm, respectively (Figure 1C,F). Moreover, the angle between the two arms is 74°, and it is identical for all Te checkmarks. Although the differences in geometry are evident, the sizes of Te nanoscale moths are virtually the same as those of Te checkmarks (Figure 1D,G), which is indicative of a synthetic relationship between them. The length of wings of Te moths and the angle between them are also 150 nm and 74 °C, respectively.

The high-resolution TEM (HRTEM) image demonstrates that the structures of single crystallite Te nanorods are of trigonal type with growth directions along the [001] direction (see Supporting Information), which are consistent with the previous reports.[40] The spacing between adjacent fringes in nanocheckmarks and nanomoths is determined to be 0.6 nm, which corresponds to the distances between (001) surfaces of Te crystals (Figure 2A,B). Similar results for crystalline spacing are also obtained by analyzing the images with fast Fourier transform (insets in Figure 2A,B). Analogously to the Te nanorods, the growth direction of either arms in nanocheckmarks or wings in nanomoths is assigned along the [001] direction. For trigonal lattice, the formula of interplanar

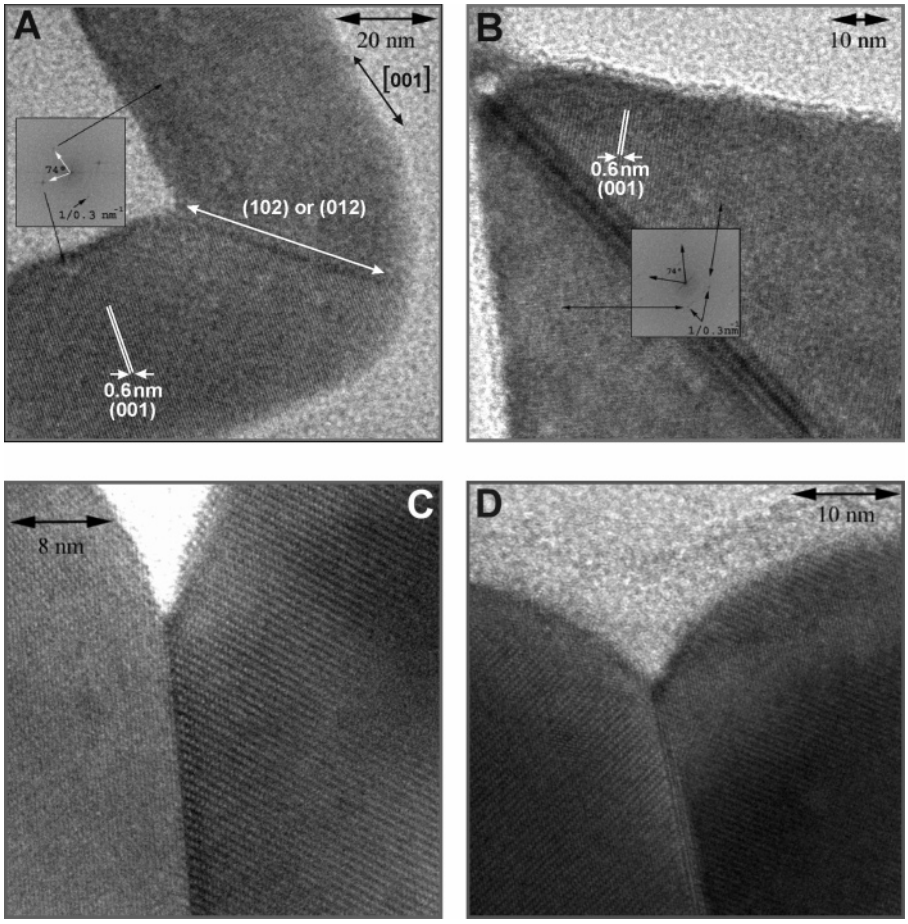

Figure 2. HRTEM images of (A) nanocheckmarks and (B) nanomoths at the junction point. (C) and (D) Angle-tilted HRTEM images of same nanomoth.

angles is expressed as:[48]

$$\cos\phi = \frac{h_1h_2 + k_1k_2 + \frac{1}{2}(h_1k_2 + h_2k) + \frac{3a^2}{4c^2}l_1l_2}{\sqrt{\left(h_1^2 + k_1^2 + h_1k_1 + \frac{3a^2}{4c^2}l_1^2\right)\left(h_2^2 + k_2^2 + h_2k_2 + \frac{3a^2}{4c^2}l_2^2\right)}}$$

For nanocheckmarks or nanomoths, $\phi = 74°/2 = 37°$, $h_1 = 0$, $k_1 = 0$, $l_1 = 1$, a and c for Te are 0.45 and 0.6 nm, respectively. Thus, if $h_2 = 0$, $l_2/k_2 = 2.05 \approx 2/1$ and the connection plane is (012). With similar calculation, the connection plane (102) is also possible. Because the contact planes in nanocheckmarks or nanomoths are determined to be (012) or (102), the calculated angles inside branched Te NCs from eq 1 should be 75.2°. The fact that the measured angles of 74° from TEM images is slightly smaller than 75.2° implies that two sides in branched Te NCs do not lie in exactly in the same plane. Angle-titled HRTEM imaging (Figure 2C,D) further confirms that the clear crystal lattices of two wings in the nanomoths or nanocheckmarks cannot be simultaneously discerned. The fold angles between two wings in Te nanomoths are estimated to be around 160° from angle-tilted HRTEM imaging, which is consistent with the value from geometrical calculation. The formation mechanism of folded sides in branched Te NCs is understood because such folded structures are capable of relaxing crystalline strain produced by the joint sides and then stabilize the structures of Te NCs. Both nanocheckmarks and nanomoths with two unique sides represent NCs with highly anisotropic structures.

Mechanism of the Nanocheckmark Formation. The conversion mechanism of Te NCs from CdTe NPs has been discussed in our previous study.[40] Briefly, EDTA can strongly bind to the surface of the depleted CdTe NPs to form $Cd(EDTA)^{2-}$ complex, and then Te^{2-} anions are gradually released into solution (eq 1). Due to strongly reducing character, Te^{2-} anions are oxidized by oxygen in the air and finally changed to Te NCs (eq 2). The shapes of Te products are observed to be highly dependent on the size of the starting CdTe NPs.

$$CdTe_{(NP)} + EDTA^{4-} \rightleftharpoons CdTe_{(NP)}Cd(EDTA)^{2-} + Te^{2-} \quad (1)$$

$$2Te^{2-} + O_2 + 2H_2O \rightarrow 2Te + 4OH^- \quad (2)$$

To explore the formation mechanism of anisotropic Te NCs, the intermediate products are evaluated by TEM imaging. At the early stage of the synthetic process, Te nanorods 8 ± 1 nm in diameter and lengths varying from 12 to 80 nm were almost exclusively detected (Figure 3B). Only occasional nanocheckmarks can be seen. The exclusive formation of the rods can be understood taking into account that the growth speed of trigonal Te crystals is much faster along the [001] rather than other directions.[42]

(48) Cullity, B. D.; Stock, S. R. *Elements of X-ray Diffraction,* 3rd ed.; Prentice Hall: Upper Saddle River, NJ, 2001; p 664.

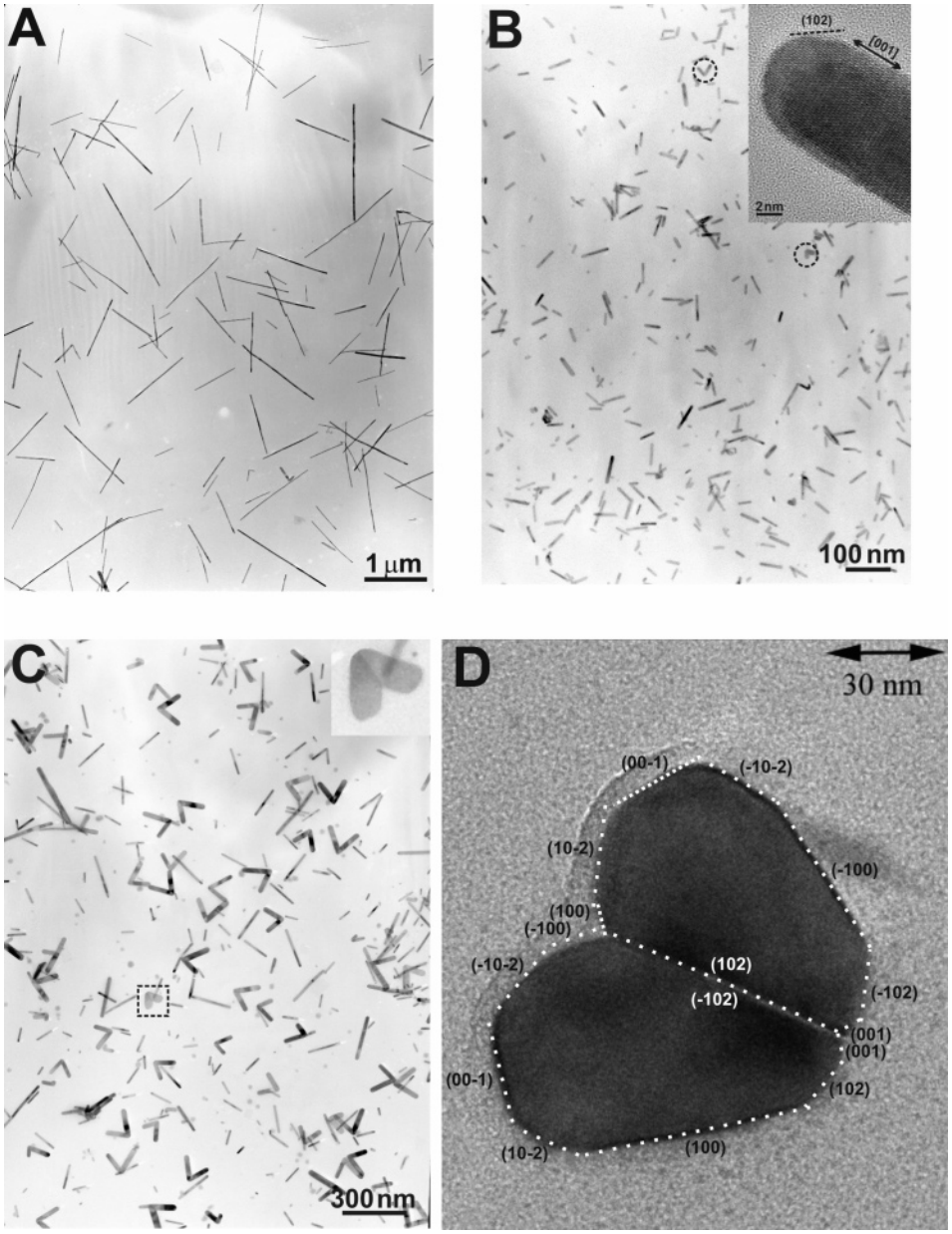

Figure 3. (A) Te nanowires from the spontaneous transformation of CdTe NPs with diameters of 5.0 nm. Evolution of self-reorganization process of CdTe NPs with diameters of 3.5 nm at (B) 6 h, (C) 2 days, and (D) 15 days. (B, inset) HRTEM images of the ends of Te nanorods. Rare nanocheckmarks in (B) are marked by circles. (C, inset) Transition state from nanocheckmarks to nanomoths. The dotted lines in (D) outline the different crystal planes on the surface of nanomoths.

After the spontaneous transformation taking place for 2 days, Te NCs with single rod shapes develop into a mixture of 68% nanorods and 32% nanocheckmarks (Figure 3C). The fact that the appearance of nanocheckmarks follows the formation of nanorods gives clear indication that the latter combine together during the reaction (Figure 3B,C), which makes them the key intermediates in the nanocheckmark formation.

So why does the growth of NCs not continue as rods? When the rate of Te crystallization slows down due to exhaustion of the monomer, the crystal growth starts competing with a different process—the process of oriented attachment, which can also be classified as self-organization of the nanorods.[49] Some of the crystal faces in the apex of the rods are (102) surfaces (inset in Figure 3B). Compared to others, the (102) surfaces on the tips of Te nanorods are the surfaces of high energy. Thus, when two Te nanorods join together via attachment of (102)

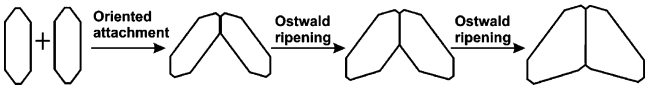

Figure 4. Proposed formation mechanism of nanomoths. Note that the scales of objects are not proportional to the real sizes of Te NCs.

surfaces (Figure 4), it results in the reduction of the total energy in the system, which apparently is the driving force of the attachment. Because the interplanar angles between (102) and (001) are 37°, the angles between the two arms in the nanocheckmarks are 75° (Figure 4), which correlates very well with experimental observations (Figure 3C). As opposed to the gradual growth of the nanorods or branched structures, here we have the case of oriented attachment of relatively large nanoscale objects driven by interparticle interactions. Unlike the cases of oriented attachment reported previously by our group,[38,39]

Talapin et al.,[20] Banfield et al.,[49] and Zitoun[15] involving NCs with spherical or cubic shapes leading to nanorods and particle chains including branched ones, oriented the attachment of Te rods results in a product with the combination of simplicity of the geometrical form and one of the extreme cases of shape anisotropy. Besides purely scientific interest as a synthetic challenge, such particles can give rise to very unusual optoelectronic properties.[50]

Along with the intrinsic affinity of high-energy surfaces to each other, two other factors may also be significant for the process of nanocheckmark formation. (1) The sizes of Te nanorods here are much smaller than for other systems.[42] This allows them to remain dispersed in the solution, which stimulates self-assembly processes. (2) The Te surface naturally has smaller surface charge density than that of binary semiconductors.

Hence, lower electrostatic repulsion between them affords successful approach of the two rods to each other followed by crystal lattice merger at the (102) or (012) connection plane.

Other Shapes. From eq 1, interplanar angles between (001) and (101) in Te NCs are calculated to be around 60°. Notice that the angles between the arms in Te Y-shaped NPs are about 120° (Figure 1E). Thus, one may conclude that the appearance of Te Ys originates from mutual attachment of three Te nanorods via (101) surfaces of their sharp tips. Because attachment through (102) surfaces is more probable than through (101) surfaces, the occurrence of Ys in the transformation products is low. This mechanism of formation of Ys correlates well both with the crystal structure of the nanorod precursors and the mechanism of nanocheckmark assembly. The formation of Te NCs with the shapes of X-marks (Figure 1F,G) is likely to result from the occasional attachment of two checkmarks or moths along opposite directions via their apexes.

Size Effect. It is important to point out the effect of particle size on the pathway of the reaction, which is fundamentally important when considering NPs as synthetic precursors of other nanostructures. When CdTe NPs, having a larger diameter of around 5.0 nm (PL maximum at 660 nm) rather than 3.5 nm, were used as precursors, only Te nanowires with diameters varying from 16 to 18 nm and lengths varying from 400 to 4000 nm were produced (Figure 3A).[40] No angled NCs were observed in this case. To understand this difference, another observation will also be helpful. The formation of intermediate rods is much slower for CdTe NPs with diameters of 5.0 nm (Figure 3A). It takes them 1−2 days to produce Te nanorods, whereas for 3.5 nm CdTe, one can see their formation in as little as 6 h. Moreover, Te nanorods from 5 nm NPs were also thicker and longer than those from 3.5 nm CdTe (Figure 3B).

The size effect in the synthesis can be explained by taking into account that partially destabilized NPs with small sizes are thermodynamically less stable than larger ones due to a higher surface-to-volume ratio and reduced density of the stabilizer shell. In the presence of EDTA compounds, the decomposition speed of L-cysteine-depleted CdTe NPs with diameters of 3.5 nm should, therefore, be faster than that of CdTe NPs with diameters of 5.0 nm. As a result, Te monomers are being formed at greater rates, which leads to a higher degree of supersaturation of Te and a greater number of Te condensation centers than for 5.0 nm CdTe. For CdTe with diameters of 3.5 nm, a high concentration of Te nuclei quickly depletes reactants and results in nanorods with both small diameters and lengths, which are easier to assemble due to fast diffusion characteristics and higher molar concentration. Finer mechanisms, such as a difference in the shape of nanorod apex, may also be in place.

Formation of Nanomoths. Along with the oriented attachment, the Ostwald ripening of different species also occurs. The theory of this process developed by Lifshitz, Slyozov, and Wagner elucidates that the growth of NCs with large sizes takes place at the expense of the dissolution of NCs with small sizes.[51,52] Compared to Te nanorods at 6 h after initiation of the transformation process (Figure 3B), the length and width of arms in nanocheckmarks increased to 120 ± 20 nm and 22 ± 3 nm, respectively. A similar increase was found for the remaining Te nanorods, and their length varied from 20 to 400 nm and diameters were 16 ± 2 nm (Figure 3C). An increase of size distribution also shows that the Ostwald ripening process takes effect in the spontaneous transformation process of Te nanorods.

Ostwald ripening apparently transforms nanocheckmarks into the nanomoths (Figure 3D). Interestingly, the speed of lateral expansion of the arms in nanocheckmarks is not equal, and inward growth speed is much faster than outward growth speed (Figure 3D and Figure 4). Fast inward growth leads to a continuous increase of contact areas along the connective {102} planes (inset in Figure 3C and Figure 3D) and, thus, decreases the lateral surface energy. The favorable inward growth eventually results in the formation of nanomoths after 15 days (Figures 3D and 4). Compared to the intermediate state for day 2 (Figure 3C), the percentage of Te nanorods in the final spontaneous transformation products decreased from 68 to 46%; the length of wings in nanomoths increased to about 150 nm with angles remaining at 74°. In agreement with the Ostwald ripening theory, the intermediate Te nanorods with small sizes were redissolved and redeposited onto NCs of large sizes. Consequently, the amount of nanorods decreased, whereas the size of nanomoths increased among the products.

Previous study has shown that chemicals may direct the growth of semiconductor NC leading to anisotropic structures.[7] To fully understand the function of EDTA, we examined the shapes of Te nanocrystals produced from the direct oxidation of Te^{2-} anions in the absence of EDTA (Figure S2A in Supporting Information).[53] We did observe the Te checkmarks with the structure similar to the products in the presence of EDTA: the length and diameter of the arms were around 150 and 30 nm, respectively, and the angle between the arms was 74°. This result confirms that the presence of EDTA only induces the spontaneous transformation of CdTe NPs rather than plays a directional role on the growth of the Te structures. We also stress that the shapes of products from the direct oxidation of Te^{2-} are not as uniform as that from EDTA-induced transformation, because the oxidation speed of Te^{2-} in the solution is too fast. The observation also shows the importance of the utilization of nanoparticles as transformation precursors, where the reaction speed and products are effectively controlled.

(49) Banfield, J. F.; Welch, S. A.; Zhang, H.; Ebert, T. T.; Penn, R. L. *Science* **2000**, *289*, 751−754.
(50) Sun, B.; Marx, E.; Greenham, N. C. *Nano Lett.* **2003**, *3*, 961−963.
(51) Lifshitz, I. M.; Slyozov, V. V. *J. Phys. Chem. Solids* **1961**, *19*, 35−50.
(52) Wagner, C. *Z. Elektrochem.* **1961**, *65*, 581−591.
(53) Pinna, N.; Weiss, K.; Urban, J.; Pileni, M. P. *Adv. Mater.* **2001**, *13*, 261−264.

Conclusion

The spontaneous transformation of stabilizer-depleted 3.5 nm CdTe NP in the presence of EDTA leads initially to the short Te nanorods, which eventually self-assemble into unusual checkmarklike Te NCs. High energy of the (012) and (102) surfaces of the tips of the short Te nanorods makes them attach preferentially to each other at this crystal face, forming assemblies of angled Te rods at a 74° angle. Subsequently, deposition of Te material between the wings of the nanocheckmarks due to the Ostwald ripening leads to the formation of nanomoths. Attachment along other surfaces leads to Y- and X-like shapes. In the Te case, we explore the formation of highly asymmetrical and branched nanocrystals via the oriented attachment of anisotropic nanorods rather than direct growth from NC seeds with high energy surfaces. This finding will help us to fully understand the intrinsic formation mechanism of branched nanocrystals as well as lead to the development of similar NP transformation strategies for other materials.

It is also important to mention that although elemental tellurium is not that toxic, a word of caution about possible toxicity of this and other nanocolloids of Te[41−43] should be made. In this respect, the synthetic route starting with nanoparticles and in aqueous media can be of the safest because no soluble or volatile Te derivatives, which present the most toxicity, are used.

Acknowledgment. This work was supported by from NSF-CAREER, NSF-Biophotonics, NIH-NASA, AFOSR, and OCAST. Z.Y.T. and N.A.K. thank Dr. Zhenli Zhang for the stimulating idea on the preliminary calculation of NR collision.

Supporting Information Available: HRTEM image of Te NR and Te NC products from direct oxidation of H2Te in the absence of EDTA and L-cysteine. This material is available free of charge via the Internet at http://pubs.acs.org.

JA0582096